Linking network- and neuron-level correlations by renormalized field theory

Michael Dick [1,2,3,*] Alexander van Meegen [1,4] and Moritz Helias [1,5]

[1]*Institute of Neuroscience and Medicine (INM-6) and Institute for Advanced Simulation (IAS-6) and JARA-Institute Brain Structure-Function Relationships (INM-10), Jülich Research Centre, 52428 Jülich, Germany*

[2]*Department of Computer Science 3 - Software Engineering, RWTH Aachen University, 52074 Aachen, Germany*

[3]*Peter Grünberg Institut (PGI-1) and Institute for Advanced Simulation (IAS-1), Jülich Research Centre, 52428 Jülich, Germany*

[4]*Institute of Zoology, University of Cologne, 50674 Cologne, Germany*

[5]*Department of Physics, Faculty 1, RWTH Aachen University, 52065 Aachen, Germany*

(Received 30 January 2024; accepted 15 August 2024; published 6 September 2024)

It is frequently hypothesized that cortical networks operate close to a critical point. Advantages of criticality include rich dynamics well suited for computation and critical slowing down, which may offer a mechanism for dynamic memory. However, mean-field approximations, while versatile and popular, inherently neglect the fluctuations responsible for such critical dynamics. Thus, a renormalized theory is necessary. We consider the Sompolinsky-Crisanti-Sommers model which displays a well studied chaotic as well as a magnetic transition. Based on the analog of a quantum effective action, we derive self-consistency equations for the first two renormalized Greens functions. Their self-consistent solution reveals a coupling between the population level activity and single neuron heterogeneity. The quantitative theory explains the population autocorrelation function, the single-unit autocorrelation function with its multiple temporal scales, and cross correlations.

DOI: 10.1103/PhysRevResearch.6.033264

I. INTRODUCTION

A. Critical neural dynamics

Both experiments and models of cortical networks suggest that the brain is operating close to a phase transition [1–4]. Indicators for this phenomenon are for example found in parallel recordings of neuronal cell cultures for which the number of coactive neurons shows power law distributions [1]. The pattern of neuronal activity, in this case referred to as an avalanche, looks identical on several length and time scales, which suggests a continuous phase transition [5]. The transition point of a continuous phase transition is synonymous with fluctuations on all time scales dominating the system's behavior. This makes it difficult to obtain systematic approximations, rendering continuous phase transitions notoriously hard to treat.

More recent work [3] suggests that the measured critical behavior could be due to the inherent subsampling in neuronal recordings which are so far only able to capture a fraction of a network's neurons. Even though this work shows that the observed critical exponents are influenced through measurement effects, it still suggests that the system is slightly subcritical. Closeness to such a transition comes with numerous benefits. Critical slowing down, the effect of increasing and, at the transition point, even diverging decay constants makes a large spectrum of time constants available to the network. This leads to optimal memory capacity as has been shown using stochastic artificial neuronal networks [6,7], and maximal computational performance [8].

So far it is unclear what phase transition the brain operates close to. However, there are two popular candidates: The first is a transition into a chaotic regime, meaning that infinitesimal changes in the neuron dynamics are progressively amplified [9–11]. The other is known as avalanchelike criticality [3,12]. Avalanches can be viewed through the lens of branching processes, treating the propagation of neuronal activity as the children and further descendants of a spontaneously emitted spike. Below criticality, each spike has on average less than one child, leading to activity being driven by external input and a quick decay of all child processes. Above criticality each neuron is on average responsible for more than one spike, leading to escalating activity. At the critical point itself, where there is on average one child spike, long transients are possible and complex behavior can emerge.

Both transitions are well studied in isolation in different models, making direct comparisons difficult. For both, the transition to chaos and avalanches, models exist which show critical behavior, but there has not yet been a study of a model supporting both phase transitions.

B. Model and renormalized theory

We want to pave the way to a comparison of the two phase transitions in this paper. To this end we focus on an adaptation of the popular and simple model by Sompolinsky, Crisanti, and Sommers [11]. It models the activity of N neurons in a randomly connected recurrent neural network. The activity of a single neuron i is denoted by $x_i(t)$ and it is governed by the

*Contact author: mi.dick@fz-juelich.de

coupled system of stochastic differential equations

$$\dot{x}_i + x_i = \sum_{j=1}^{N} J_{ij}\phi_j + \xi_i, \tag{1}$$

where we use the abbreviation $\phi_i \equiv \phi(x_i)$ and the driving noise ξ_i is assumed to be Gaussian white noise with zero mean and covariance $\langle \xi_i(t)\xi_j(s)\rangle = D\,\delta_{ij}\,\delta(t-s)$. Here ϕ is an arbitrary activation function for most of this paper; in simulations we chose an error function $\phi(x) = \mathrm{erf}(\frac{\sqrt{\pi}}{2}x) = \int_0^x e^{-\frac{\pi}{4}z^2}\,dz$ where the scaling ensures that the slope at the origin is unity. In the absence of the right-hand side in (1), the activity decays exponentially with unit time constant. The right-hand side represents the input to the neuron. The first part comes from all other neurons determined via the activation function ϕ and the connectivity J, whose $N \times N$ weights are distributed according to a Gaussian with mean $\bar{g}/N$ (which is often set to zero) and variance g^2/N. We will refer to $\bar{g}$ as the mean and g^2 as the variance of the connectivity as the factor N^{-1} is simply chosen such that mean and fluctuations of the input to a neuron do not scale with the total number of neurons. The second source of input is a random white noise ξ_i with noise intensity D modeling external input from other brain areas.

To link this model to the two forms of criticality mentioned above, we consider $\bar{g}$ as the control parameter for avalanche-like activity; if nonzero and positive it controls the strength by which the average population activity at a certain instant excites and maintains the activity at the next point in time. More formally, in the limit of large N, the parameter $\bar{g}$ controls a single real outlier eigenvalue of the connectivity matrix, $\bar{\lambda} = \bar{g}$ [13,14], with corresponding eigenvector $(1, \ldots, 1)$. The latter is a mode in which all neurons act in unison, a cartoon of what happens in a neuronal avalanche. If this eigenvalue $\bar{\lambda}$ crosses unity, the silent fixed point of the noiseless ($D = 0$) model becomes unstable in this very direction [15]. The transition to chaos, in contrast, is predominantly controlled by the parameter g. Studying the eigenvalues of the connectivity, g controls the radius of the bulk of eigenvalues which are uniformly distributed in a circle with radius g around the origin of the complex plane. Again, a critical point is reached if this radius reaches unity, because then all eigenmodes with $\Re(\lambda_i) \simeq 1$ show critically slow dynamics. In the noiseless case $D = 0$ (and for $\bar{g} = 0$) this points marks the onset of chaotic dynamics [11].

The theoretical approach to the disordered system described by (1) is based on mean-field approximations on auxiliary fields like

$$R(t) := \frac{\bar{g}}{N}\sum_{j=1}^{N}\phi_j(t), \tag{2}$$

$$Q(s,t) := \frac{g^2}{N}\sum_{j=1}^{N}\phi_j(s)\phi_j(t), \tag{3}$$

since they give a way to obtain an effective low-dimensional set of equations describing the collective behavior. This approach has been used to show a transition to chaos with g^2 acting as control parameter [11], which has been studied extensively [9,16]. As discussed above, the mean $\bar{g}$ of the connectivity can also take the form of a control parameter [15]: as seen empirically in Fig. 1(a) the network exposes large variance in its population-averaged activity R as $\bar{g}$ approaches the transition point given by $\bar{g}$ close to unity for $g < 1$. Close to this criticality the fluctuations of R will influence Q as can be seen in Fig. 1(b), leading on average to a larger autocorrelation. The parabolic shape can be understood by interpreting the sum in Eq. (2) and the equal time case of Eq. (3) as an empirical average, thus splitting $Q(t,t)$ into a sum of $\frac{g^2}{\bar{g}^2}R(t)^2$ and a term given by the second cumulant of ϕ. In this work we derive an analytical way to analyze the network's behavior close to this transition using $\bar{g}$ as a control parameter, taking into account the fluctuations of population-averaged activity and its effect on the autocorrelation function.

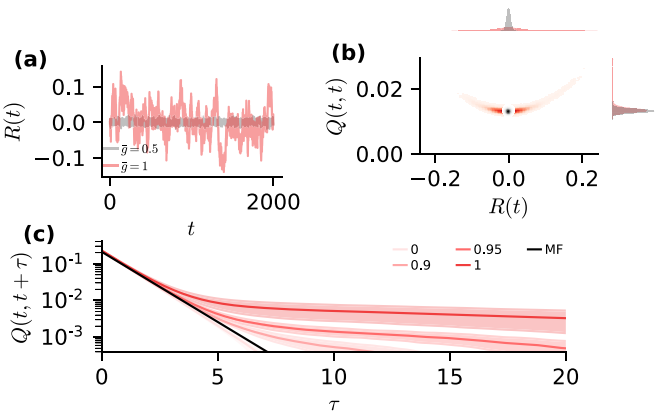

FIG. 1. (a) Population-averaged activity $R(t)$ for $\bar{g} = 0.5$ (gray) and $\bar{g} = 1$ (red). (b) Auxiliary fields Q and R, proportional to population-averaged output autocorrelation and activity, respectively, binned for each point in time. (c) Time-lagged, population-averaged, stationary autocorrelation $Q(t, t+\tau)$ simulated for different values of $\bar{g}$ (shades of red) for multiple seeds (shaded background shows the standard deviation) and mean field prediction (black) plotted logarithmically. Remaining network parameters: $\phi(x) = \mathrm{erf}(\frac{\sqrt{\pi}}{2}x)$, $N = 1000$, $g = 0.5$, and $D = 0.1$.

The proper treatment of fluctuations comes with some technical difficulties. Mean-field approaches, albeit being very popular in the field [9,17–19], neglect fluctuations of the auxiliary fields. This effect can be seen in Fig. 1(c), which shows the population averaged autocorrelation simulated for several values of $\bar{g}$ close to unity compared to the analytical mean-field solution, which corresponds in this case to a network with $\bar{g} = 0$. One clearly sees that the mean-field results (black) describes only a simple exponential decay (for a linear network the time constant is $\sqrt{1-g^2}^{-1}$, see Appendix D; for a nonlinear network the time constant is captured by the mean-field theory, see Appendix A). This is insufficient to quantitatively capture the slow tail of the autocorrelation function whose time constant grows with rising $\bar{g}$ (plotted in shades of red).

One way of taking these fluctuations into account is by means of Legendre transformation methods [20]. These provide a way to derive a set of self-consistent equations that resum these fluctuations and are therefore able to describe the observed behavior.

C. Outline

We will derive a set of self-consistent equations for the mean and the fluctuations of the auxiliary fields (2) and (3). Such self-consistent schemes are commonplace in other fields of physics [20,21]. These approximations are typically formulated in the language of a field theory. As a first step, we therefore formulate the dynamical equations in this language. Initially we will leave the activation function ϕ general; all we ask of it is to vanish at zero and to possess a Fourier transform. This set of self-consistency equations in particular exposes how the fluctuations of the population-averaged activity R influence the population-averaged autocorrelation Q, as shown empirically in Figs. 1(b) and 1(c). The theory also allows us to compute pairwise correlations averaged across all pairs of neurons in the network. Lastly, the theory proposes that stimulations that excite the population-averaged activity R also influence the variance of the response across neurons, as measured by Q.

II. SELF-CONSISTENT SECOND-ORDER STATISTICS

A. Action for Auxiliary Fields

First, we translate Eq. (1) into the language of field theory. To this end, it is instructive to first look at the noise expectation value of an operator $G[\boldsymbol{x}]$ constrained to the dynamics of Eq. (1). This can be achieved with help of the Martin-Siggia-Rose-de Dominicis-Janssen formalism [22–24] (for pedagogic reviews see Refs. [25–27]) and results in

$$\begin{aligned}\langle G[\boldsymbol{x}]\rangle_{\boldsymbol{x}|\boldsymbol{J}} &= \int_{\boldsymbol{x}} \langle \delta[\dot{\boldsymbol{x}} + \boldsymbol{x} - \boldsymbol{J}\boldsymbol{\phi}(\boldsymbol{x}) - \boldsymbol{\xi}]\rangle_{\boldsymbol{\xi}}\, G[\boldsymbol{x}] \\ &= \int_{\boldsymbol{x},\tilde{\boldsymbol{x}}} e^{S_0[\boldsymbol{x},\tilde{\boldsymbol{x}}] - \tilde{\boldsymbol{x}}^T \boldsymbol{J}\boldsymbol{\phi}(\boldsymbol{x})}\, G[\boldsymbol{x}]. \end{aligned} \tag{4}$$

Here, $\int_{\boldsymbol{x}}$ denotes an integral over the trajectories of all neurons and we used $\delta(x) = \frac{1}{2\pi i}\int_{-i\infty}^{i\infty} e^{\tilde{x}x}\, d\tilde{x}$ for every time step and neuron and defined the action

$$S_0[\boldsymbol{x},\tilde{\boldsymbol{x}}] := \tilde{\boldsymbol{x}}^{\mathrm{T}}(\partial_t + 1)\,\boldsymbol{x} + \frac{D}{2}\tilde{\boldsymbol{x}}^{\mathrm{T}}\tilde{\boldsymbol{x}} \tag{5}$$

with the short hand notations $\boldsymbol{a}^{\mathrm{T}}\boldsymbol{b} = \sum_{i=1}^{N}\int_0^t ds\, a_i(s)b_i(s)$ and $\boldsymbol{a}^{\mathrm{T}}\boldsymbol{M}\boldsymbol{b} = \sum_{i,j=1}^{N}\int_0^t ds\, a_i(s)M_{ij}b_j(s)$.

This allows the definition of a characteristic functional $Z[\boldsymbol{l}]$ by setting $G[\boldsymbol{x}] = \exp(\boldsymbol{l}^{\mathrm{T}}\boldsymbol{x})$. The source $\boldsymbol{l}$ in the exponent allows us to take derivatives which in turn yield properly normalized moments after evaluating at the physical value $\boldsymbol{l} = 0$ of the sources. These sources need not be linear in $\boldsymbol{x}$ and could even couple to entirely different quantities. Until we need them we will leave them out and first consider only the partition function.

Eventually, we are interested in self-averaging quantities like the mean (2) and the autocorrelation function (3); thus, we further average over realizations of the connectivity $J_{ij} \overset{\text{i.i.d.}}{\sim} \mathcal{N}(\bar{g}/N, g^2/N)$ which only affects the term $-\tilde{\boldsymbol{x}}^{\mathrm{T}}\boldsymbol{J}\boldsymbol{\phi}(\boldsymbol{x})$ and yields

$$\langle e^{-\tilde{\boldsymbol{x}}^{\mathrm{T}}\boldsymbol{J}\boldsymbol{\phi}(\boldsymbol{x})}\rangle_{\boldsymbol{J}} = \int_y \exp\left(\frac{N}{2}\,y^{\mathrm{T}}Ky + \sum_{i=1}^{N} y^{\mathrm{T}} f[z_i]\right). \tag{6}$$

Here, we introduced the population-averaged auxiliary fields R defined in Eq. (2) and Q defined in Eq. (3) via Hubbard-Stratonovich transformations and their respective response fields $\tilde{R}$ and $\tilde{Q}$ analogously to the introduction of $\tilde{\boldsymbol{x}}$. Furthermore, we introduced several short-hand notations: First, we denote $\boldsymbol{x}$ and $\tilde{\boldsymbol{x}}$ in combination as $\boldsymbol{z} = (\boldsymbol{x}, \tilde{\boldsymbol{x}})$ and $R, \tilde{R}, Q$, and $\tilde{Q}$ in combination as $y = (R, \tilde{R}, Q, \tilde{Q})$. Second, we abbreviate $y^{\mathrm{T}} f[z_i] = -\tilde{x}_i^{\mathrm{T}} R - \bar{g}\boldsymbol{\phi}_i^{\mathrm{T}}\tilde{R} + \frac{1}{2}\tilde{x}_i^{\mathrm{T}} Q\tilde{x}_i - g^2\boldsymbol{\phi}_i^{\mathrm{T}}\tilde{Q}\boldsymbol{\phi}_i$. Third, we define $K = \left(\begin{smallmatrix}\sigma_x & 0\\ 0 & \sigma_x\end{smallmatrix}\right)$ where $\sigma_x = \left(\begin{smallmatrix}0 & 1\\ 1 & 0\end{smallmatrix}\right)$, leading to $\frac{1}{2}\,y^{\mathrm{T}}Ky = \tilde{R}^{\mathrm{T}}R + \tilde{Q}^{\mathrm{T}}Q$. In summary, the introduced notation allow us to write

$$\langle\langle G(\boldsymbol{x})\rangle_{\boldsymbol{x}|\boldsymbol{J}}\rangle_{\boldsymbol{J}} = \int_y e^{\frac{N}{2}\,y^{\mathrm{T}}Ky} \prod_{i=1}^{N}\int_{z_i} e^{S_0[z_i] + y^{\mathrm{T}} f[z_i]}\, G(x_i)$$

for any factorizing $G(\boldsymbol{x}) = \prod_{i=1}^{N} G(x_i)$.

We see that the part of the partition function that describes individual neurons factorizes into N identical factors. This leaves a partition function for the four auxiliary fields interacting with a single neuron

$$\int_y e^{\frac{N}{2}\,y^{\mathrm{T}}Ky} \prod_{i=1}^{N}\int_{z_i} e^{S_0[z_i] + y^{\mathrm{T}} f[z_i]} = \int_y \exp\left(N\,S[y]\right),$$

where we defined the action for the auxiliary fields as

$$S[y] := \frac{1}{2}y^{\mathrm{T}}Ky + \mathcal{W}[y], \tag{7}$$

$$\mathcal{W}[y] := \ln \int_z \exp(S_0[z] + y^{\mathrm{T}} f[z]), \tag{8}$$

reducing the dimensionality of the problem from N neurons to the six fields y and z. We note that $\mathcal{W}[y]$ has the form of a cumulant-generating functional for $f[z]$.

B. Mean-Field Phase Diagram

As the lowest order (mean-field) approximation one can treat the path integrals $\int_y$ in saddle point approximation, replacing the auxiliary fields with their most likely values obtained from the condition $\delta S[y]/\delta y_i \overset{!}{=} 0$, which yields [7,15,16,27]

$$\begin{aligned} y^* &= (R^*, \tilde{R}^*, Q^*, \tilde{Q}^*) \\ &= (\bar{g}\mu_\phi, 0, g^2 C_{\phi\phi}, 0), \end{aligned}$$

with

$$\mu_\phi(t) = \langle\phi(t)\rangle,$$

$$C_{\phi\phi}(t,s) = \langle\phi^2(s,t)\rangle,$$

where $\langle\ldots\rangle$ is the measure determined by the action (7) and $\phi^2(s,t) := \phi(t)\phi(s)$.

We are now left with path integral for a single neuron and its response field which corresponds to the stochastic differential equation

$$\dot{x} + x = \xi + \eta, \tag{9}$$

where η is a Gaussian Process with

$$\langle\langle\eta(t)\rangle\rangle = \bar{g}\mu_\phi(t), \tag{10}$$

$$\langle\langle\eta(s)\eta(t)\rangle\rangle = g^2 C_{\phi\phi}(s,t), \tag{11}$$

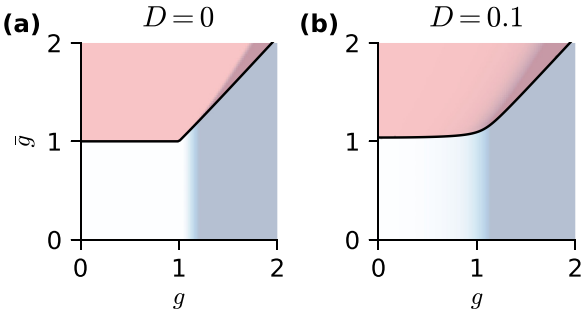

FIG. 2. Mean-field phase diagram spanned by $\bar{g}$ and g for (a) the noiseless case ($D = 0$) and (b) noise-driven dynamics ($D = 0.1$). The red shading quantifies the absolute population activity $|R(t)|$, which is the order parameter for ferromagnetic activity, and the gray shading quantifies the dynamic variability $Q(t, t)$, which for $D = 0$ is the order parameter indicating the onset of chaotic activity. Above the black curves, the population activity R becomes nonzero. The dynamic variability $Q(t, t)$ does not vanish in the presence of noise.

where we use $\langle\langle \ldots \rangle\rangle$ to denote cumulants (connected correlation functions). For an error function as the nonlinearity these expectations can be calculated analytically in terms of statistics of the neuron activity [28]. Thus Eq. (9) can be solved efficiently in a self-consistent manner.

For the case of vanishing noise ($D = 0$) the saddle-point approximation recovers the phase diagram from [15, Fig. 1B], see also Fig. 2(a): The system exhibits a transition from a state with a vanishing order parameter $R = 0$ to a state with a broken symmetry where $|R| > 0$ at a critical value $\bar{g} = \bar{g}_c$. For the case with noise ($D > 0$), the point of transition in addition depends on the noise amplitude $\bar{g} = \bar{g}_c(g, D)$; see Eq. (A6) for an explicit expression for $D = D(\bar{g}_c, g)$ which can be solved for $\bar{g}_c = \bar{g}_c(g, D)$.

C. Equations of State to 1-loop Order

We are especially interested in the transition to structured activity $|R| > 0$ driven by the mean connectivity $\bar{g}$. We expect this transition to be accompanied by fluctuations of the auxiliary field (2) and thus aim to derive a description treating population-wide fluctuations systematically.

To build intuition, we first perform a straightforward fluctuation expansion. To this end we add a source term $\phi^{\mathrm{T}}\ell\phi$ to (8) defining $S_\ell[y]$ analogously to Eq. (7) and the corresponding cumulant generating functional $\hat{W}[\ell] = \ln \int_y e^{NS_\ell[y]}$. Now expanding around y^*_ℓ defined by $S'_\ell[y^*_\ell] = \delta S_\ell[y]/\delta y_i|_{y^*_\ell} \stackrel{!}{=} 0$ to second order we find

$$\begin{aligned}\hat{W}[\ell] &= \ln \int_y e^{NS_\ell[y]} \\ &= \ln \int_{\delta y} e^{NS_\ell[y^*_\ell] + \frac{1}{2}\delta y^2 S''_\ell[y^*_\ell]} \\ &= NS_\ell[y^*_\ell] - \frac{1}{2}\mathrm{tr}\ln(-S''_\ell[y^*_\ell]) + \text{const.} \end{aligned} \tag{12}$$

From here we obtain the single unit correlations as $\langle\phi\phi\rangle = N^{-1}\frac{\partial\hat{W}[\ell]}{\partial\ell}|_{\ell=0}$, where we can easily see that the first term of Eq. (12) yields the mean-field result, while the second term

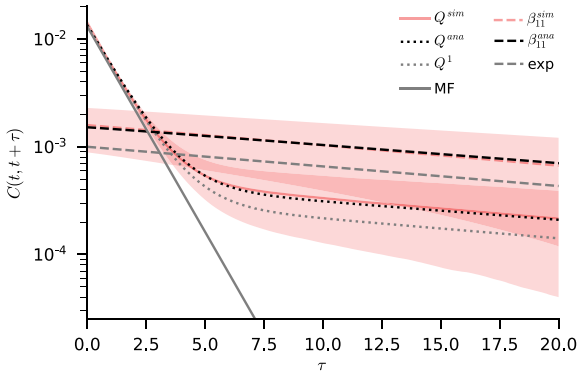

FIG. 3. Time lagged population-averaged autocorrelation $Q(t, t + \tau)$ (3) simulated (red) with standard deviation across seeds (shaded), mean-field theory (gray), fluctuation expansion (12) (gray dotted) and self-consistent solution (25) (black dotted) together with autocorrelation $\langle\langle R(t + \tau)R(t)\rangle\rangle = \beta_{11}(\tau)$ of population-averaged activity R (2) (dashed, self-consistent in black, empirical in red, exponential decay with time scale $(1 - \bar{g}\langle\phi'\rangle)^{-1}$ in gray) plotted logarithmically for $\bar{g} = 1.0$. Other parameters as in Fig. 1.

leads to finite size corrections suppressed by $1/N$ compared to the first term. However, this approximation neglects the feedback of the single unit autocorrelation on the population level and thus underestimates the strength of the correction (see Fig. 3). The approach based on a loop expansion developed below will take this feedback between single-unit and network-level into account. Technically, the improvement due the loop expansion results from a resummation of diagrams [20,29].

The population level activity is captured by the auxiliary fields. It is thus natural to introduce sources for these fields and for their square to measure their fluctuations. This leads us to the definition of a moment generating functional

$$Z[j, k] = \int_y e^{N\mathcal{W}[y] + j^{\mathrm{T}}y + \frac{1}{2}y^{\mathrm{T}}k^{\mathrm{T}}y}, \tag{13}$$

which yields the first and second moment of y upon differentiation by j and k, respectively, at the physically relevant value of the sources $j = 0$ and $k = NK$, by comparison to (7). Our aim is to obtain self-consistency equations for the first two moments. It is, therefore, helpful to define an ensemble where these two moments are fixed. This is achieved by performing a second-order Legendre transform to the effective action

$$\begin{aligned}\Gamma[\alpha_1, \alpha_2] &= \mathrm{extr}_{j,k}\, j^{\mathrm{T}}\alpha_1 + \frac{1}{2}k^{\mathrm{T}}\alpha_2 - \ln Z[j, k] \\ &= \mathrm{extr}_{j,k} - \ln \int_y e^{N\mathcal{W}[y] + j^{\mathrm{T}}(y-\alpha_1) + \frac{1}{2}k^{\mathrm{T}}(y^2-\alpha_2)},\end{aligned}$$

which fixes the system's first two moments α_1, α_2 of the auxiliary fields y; here $k^{\mathrm{T}}y^2$ is meant as a bilinear form in y. The equations of state then yield self-consistency equations

$$\begin{aligned}\frac{\delta\Gamma}{\delta\alpha_1} &= j = 0, \\ \frac{\delta\Gamma}{\delta\alpha_2} &= \frac{1}{2}k = \frac{1}{2}NK.\end{aligned} \tag{14}$$

Below, we will perform a fluctuation expansion of Γ. To ensure that only connected diagrams appear in the expansion [20], we describe the system via its cumulants $\beta_1 = \alpha_1$ and $\beta_2 = \alpha_2 - \alpha_1^2$ and define an effective action in these new coordinates (see Appendix B)

$$\Gamma[\beta_1, \beta_2] = \operatorname{extr}_{\hat{j},k} - \ln \int_y e^{N\mathcal{W}[y] + \hat{j}^{\mathrm{T}}(y-\beta_1) + \frac{1}{2}k^{\mathrm{T}}[(y-\beta_1)^2 - \beta_2]},$$

where $\hat{j} := j + k\beta_1$. Following Vasiliev [20] we here use the notation of α_n for the nth moment and β_n for the nth cumulant. We thus have $(\beta_1)_1 = \langle\langle R\rangle\rangle =: R^*$ and $(\beta_1)_3 = \langle\langle Q\rangle\rangle =: Q^*$. The other two components of β_1 are zero, as they are cumulants of response fields. For β_2 we will use the notation $\beta_{ij} = (\beta_2)_{ij}$ as it comes up frequently. So we have β_{11} as the autocorrelation of R, β_{12} and β_{21} as its response functions and again $\beta_{22} = 0$ as a cumulant of only response fields. The equations of state (14) in the new coordinates take the form

$$\frac{\delta\Gamma[\beta_1, \beta_2]}{\delta\beta_1} = j + \beta_1 k = \beta_1 NK, \tag{15}$$

$$\frac{\delta\Gamma[\beta_1, \beta_2]}{\delta\beta_2} = \frac{1}{2}k = \frac{1}{2}NK. \tag{16}$$

Writing the problem in this way uses the yet unknown fluctuation-corrected self-consistent values for the first and second-order statistics which become accessible via the equations of state.

Solving the equations of state is difficult in general but as $S[y] \propto N$ a diagrammatic expansion will contain a factor N^{-1} for each loop in the diagram, making a loop-wise expansion meaningful. Up to one-loop order and neglecting additive constants we get by expanding $\mathcal{W}[y] = \mathcal{W}[\beta_1] + \frac{1}{2}(y-\beta_1)^{\mathrm{T}}\mathcal{W}^{(2)}[\beta_1](y-\beta_1)$ and performing the resulting Gaussian integral over the fluctuations $\delta y = y - \beta_1$

$$\begin{aligned}\Gamma_{1\text{-loop}}[\beta_1, \beta_2] = &- N\,\mathcal{W}[\beta_1] + \tfrac{1}{2}k^{\mathrm{T}}\beta_2 \\ &+ \tfrac{1}{2}\ln\det(-N\mathcal{W}^{(2)}[\beta_1] - k).\end{aligned}$$

Note that the terms linear in the fluctuations do not contribute to one-loop order. Using the stationarity condition $\frac{\delta}{\delta k}\Gamma_{1\text{-loop}}[\beta_1, \beta_2] = 0$, we obtain $\beta_2 = (-N\mathcal{W}^{(2)}[\beta_1] - k)^{-1}$ which simplifies the effective action to

$$\begin{aligned}\Gamma_{1\text{-loop}}[\beta_1, \beta_2] = &- N\,\mathcal{W}[\beta_1] - \tfrac{1}{2}N\,\mathcal{W}^{(2)}[\beta_1]^{\mathrm{T}}\beta_2 \\ &- \tfrac{1}{2}\ln\det(\beta_2),\end{aligned}$$

where we suppressed the inconsequential constant $-\frac{1}{2}\mathrm{tr}\,\mathbb{I}$. Here we already see the finite size corrections. While the first term, which is equivalent to the saddle point approximation, is of order N, the order of the second term depends on the order of β_2, which as we will later see will be N^{-1}. This makes this term of order one, just like the last term. Up to one-loop order and evaluated at their true value $j = 0$ and $k = NK$ the first equation of state (15) reads

$$\begin{aligned}\frac{\delta\Gamma_{1\text{-loop}}[\beta_1, \beta_2]}{\delta\beta_1} &= -N\,\mathcal{W}^{(1)}[\beta_1] - \frac{1}{2}N\mathcal{W}^{(3)}[\beta_1]^{\mathrm{T}}\beta_2 \\ &= \beta_1 N\,K.\end{aligned} \tag{17}$$

The second equation of state (16) is

$$\begin{aligned}\frac{\delta\Gamma_{1\text{-loop}}[\beta_1, \beta_2]}{\delta\beta_2} &= -\frac{1}{2}N\,\mathcal{W}^{(2)}[\beta_1] - \frac{1}{2}\beta_2^{-1} \\ &= \frac{1}{2}NK.\end{aligned} \tag{18}$$

The derivatives of $\mathcal{W}$ evaluated at $y = \beta_1$ by Eq. (8) take the form of the cumulants of $f[z]$ taken with the measure

$$P[z] \propto e^{S_0[z] + \beta_1^{\mathrm{T}} f[z]}. \tag{19}$$

Two things are important to note about this measure. First, β_1 has only two nonvanishing components. This means we get $\beta_1^{\mathrm{T}} f[z] = -R^{*\mathrm{T}}\tilde{x} + \frac{1}{2}\tilde{x}^{\mathrm{T}}Q^*\tilde{x}$ which is at most quadratic in z, as both terms containing $\phi(x)$ vanish. Therefore, the measure (19) is Gaussian which greatly simplifies the calculations. Second, this measure is not determined by the fluctuation-corrected statistics but the saddle-point values of the auxiliary fields: R^* and Q^*. To avoid confusion, we will use the subscript $*$ for cumulants taken with measure (19).

D. Evaluating the 1-loop Equations of State

We will separate the different contributions to the cumulant by commas due to the third and fourth entry of f consisting of two parts with two time arguments. A quick example of this necessity is the comparison between $\langle\langle f_4(s,t)[z]\rangle\rangle_*$ and $\langle\langle f_2[z](s), f_2[z](t)\rangle\rangle_*$ because without a separator they look identical: $\langle\langle\phi(s)\phi(t)\rangle\rangle_*$ (neglecting prefactors) but this is of course misleading.

With this notation we now close the self-consistency loop by solving the equations of state for the cumulants. We will start by solving Eq. (18) for β_2 which appears linearly,

$$\left(\beta_2^{-1}\right)_{i,j} = N\,K_{i,j} + N\,\langle\langle f[z]_i, f[z]_j\rangle\rangle_*. \tag{20}$$

Working under the assumption of a point symmetric activation functions and under the assumption that $\langle x\rangle = 0$, we have $\langle\langle\phi(x)\rangle\rangle_* = 0$ as well as $\langle\langle\phi^3(x)\rangle\rangle_* = 0$ and $\langle\langle\phi, \tilde{x}\tilde{x}\rangle\rangle_* = 0$; the latter is the response of the mean $\langle\phi\rangle$ to a perturbation of the variance of x. Taking into account that any expectation value solely composed of powers of $\tilde{x}$ must vanish, we see that $\langle\langle f[z]_i, f[z]_j\rangle\rangle_* = 0$ if $i \in \{1,2\}$ and $j \in \{3,4\}$ or vice versa. Due to the block-diagonal shape of K, β_2^{-1} is block-diagonal as well. We can therefore invert these blocks independently. The upper left block of Eq. (20) takes the form

$$\begin{aligned}\left(\beta_2^{-1}\right)_{11}(t,s) &= N\,\langle\langle\tilde{x}(t), \tilde{x}(s)\rangle\rangle_* = 0, \\ \left(\beta_2^{-1}\right)_{12}(t,s) &= N\delta(t-s) + N\bar{g}\,\langle\tilde{x}(t)x(s)\rangle_*\langle\phi'\rangle_*, \\ \left(\beta_2^{-1}\right)_{21}(t,s) &= N\delta(t-s) + N\bar{g}\,\langle\tilde{x}(s)x(t)\rangle_*\langle\phi'\rangle_*, \\ \left(\beta_2^{-1}\right)_{22}(t,s) &= N\bar{g}^2\,\langle\langle\phi(t), \phi(s)\rangle\rangle_*,\end{aligned}$$

which we can rewrite in momentum-space

$$\begin{aligned}\left(\beta_2^{-1}\right)_{21}(\omega) &= N - N\bar{g}\frac{\langle\phi'\rangle_*}{1+i\omega}, \\ \left(\beta_2^{-1}\right)_{12}(\omega) &= N - N\bar{g}\frac{\langle\phi'\rangle_*}{1-i\omega}, \\ \left(\beta_2^{-1}\right)_{22}(\omega) &= N\bar{g}^2\langle\langle\phi, \phi\rangle\rangle_*(\omega).\end{aligned}$$

Here we used the results from Appendix C to rewrite $\langle\langle \tilde{x}\phi\rangle\rangle_* = \langle\phi'\rangle_*\langle\tilde{x}x\rangle_*$ and the Fourier representation of the response functions $\langle\tilde{x}x\rangle_*(\omega) = -1/(1+i\omega)$, i.e., the response of a neuron to a δ perturbation with respect to the measure (19), which has the same form as for isolated neuron, because the additional term $\beta_1^{\mathrm{T}} f(z)$ in the action corresponds to an additional input which does not affect the response. Finally, we invert this matrix [greatly simplified due to $(\beta_2^{-1})_{11}(t,s) = 0$] to find

$$\begin{aligned}\beta_{12}(\omega) &= \left(\left(\beta_2^{-1}\right)_{21}(\omega)\right)^{-1} \\ &= N^{-1}\,\frac{1+i\omega}{1-\bar{g}\langle\phi'\rangle+i\omega}, \qquad (21)\\ \beta_{21}(\omega) &= \beta_{12}(-\omega), \qquad (22)\end{aligned}$$

$$\begin{aligned}\beta_{11}(\omega) &= \beta_{12}(\omega)\,(\beta^{-1})_{22}(\omega)\,\beta_{21}(\omega)\\ &= \frac{1+\omega^2}{(1-\bar{g}\langle\phi'\rangle)^2+\omega^2}\,\frac{\bar{g}^2}{N}\,\langle\langle\phi,\phi\rangle\rangle_*(\omega). \qquad (23)\end{aligned}$$

Here we see the first clear sign of the emerging large time constant in $\beta_{11}(\omega)$. When $\bar{g}$ approaches $\langle\phi'\rangle^{-1}$ a pole emerges at $\omega = 0$. This implies that $\beta_{11}(\tau)$, the autocorrelation of the population averaged activity, decays slower and slower to zero as a function of $t-s$ and thus obtains a large decay constant: the first part of the population activity autocorrelation (23) contributes a term decaying with a time constant of $(1-\bar{g}\langle\phi'\rangle)^{-1}$. We can also see that $\beta_{22} = 0$ as it should since it is the second cumulant of $\tilde{R}$ which is a response field. By the same argument $\beta_{44} = \langle\langle\tilde{Q}^2\rangle\rangle$ must vanish. This implies that one could apply the same method to invert the lower right block; here we refrain from doing this because our main interest lies in studying the effect of fluctuations of the population-averaged activity R, which is described by the upper left block.

Next, we solve for the mean via the first equation of state (17) which takes the form

$$(K\beta_1)_i = -\langle\langle f_i[z]\rangle\rangle_* - \frac{1}{2}\sum_{l,m\in\underline{4}}\langle\langle f_i[z], f_l[z], f_m[z]\rangle\rangle_*\beta_{lm}, \qquad (24)$$

where $\underline{4} = \{1,2,3,4\}$. Note that the multiplication with K, does nothing but switch indices $1\leftrightarrow 2$ and $3\leftrightarrow 4$. In principle, Eq. (24) determines all mean values of the population dynamic. We are, however, especially interested in corrections to R and Q, the auxiliary fields used in the mean field. Thus, we consider the cases $i=2$ and $i=4$. The first shows that the correction on the population activity R caused by its own fluctuations β_{11} is mediated by $\langle\langle\phi\tilde{x}\tilde{x}\rangle\rangle \propto \langle\phi''\rangle$ (for details see Appendix C, which vanishes in the paramagnetic regime. This means that that there is no influence of fluctuations of R on the transition to the ferromagnetic state. For the second we need the product of β_2 and the third cumulant of f. This leads to 16 different combinations of l and m. As discussed above, β_2 has several vanishing entries: the off-diagonal blocks and the auto-correlations of response fields, β_{22} and β_{44}. This already reduces the number of terms from 16 to 6. Additionally, the term involving

$$\langle\langle f_4[z], f_3[z], f_3[z]\rangle\rangle_* \propto \langle\langle\phi^2,\tilde{x}^2,\tilde{x}^2\rangle\rangle_*$$

vanishes. This can be shown by methods from Appendix C, which work similar to Wick's theorem to express those moments as a polynomial of second cumulants of x and $\tilde{x}$, results in a formula where every term is at least proportional to $\langle\langle\tilde{x},\tilde{x}\rangle\rangle_* = 0$.

For the fourth component of Eq. (24), this leaves us with

$$\begin{aligned}Q^*(s,t) &= (\beta_1(s,t))_3 = (K\beta_1(s,t))_4 \qquad (25)\\ &= g^2\langle\langle\phi^2(s,t)\rangle\rangle_* \qquad (26)\\ &\quad + \frac{1}{2}g^2\int_{u,v}\langle\langle\phi^2(s,t),\tilde{x}(u),\tilde{x}(v)\rangle\rangle_*\beta_{11}(u,v) \qquad (27)\\ &\quad + g^2\bar{g}\int_{u,v}\langle\langle\phi^2(s,t),\tilde{x}(u),\phi(v)\rangle\rangle_*\beta_{12}(u,v) \qquad (28)\\ &\quad - \frac{g^4}{2}\int_{u_{1,2},v_{1,2}}\langle\langle\phi^2(s,t),\tilde{x}^2(u_1,u_2),\phi^2(v_1,v_2)\rangle\rangle_* \\ &\qquad \times\beta_{34}(u_1,u_2,v_1,v_2). \qquad (29)\end{aligned}$$

This equation lends itself nicely to interpretation using the intuitive picture of a mean-field neuron embedded in a bath of activity due to the network (akin to the cavity method [30]). The first contribution, Eq. (26), is identical to the mean-field approximation. The next contribution (27) contains β_{11}, the autocorrelation of the population averaged activity R. This term can be interpreted as the effect of fluctuations of R measured by β_{11} contributing to the variance of the input of the representative mean-field neuron. Term (28) shows how a fluctuation of the neuronal activity $\phi(v)$ is echoed in the network and transmitted back by the response function β_{12} of the bath, affecting the mean input by coupling to $\tilde{x}(u)$ which, in turn, modifies the variance of the mean-field neuron's input by changing the second moment $\langle\phi^2(s,t)\rangle$. Similarly Eq. (29) shows an echo effect: A fluctuation of $\phi^2(v_1,v_2)$ propagates through the bath with the response $\beta_{34}(u_1,u_2,v_1,v_2)$ to time points u_1,u_2 and causes a change of the variance in the input of the mean-field neuron by coupling to $\tilde{x}^2(u_1,u_2)$, which in turn affects $\langle\phi^2(s,t)\rangle$. Note that all β_{ij} come with an factor $1/N$ as can be seen from Eq. (20) or more explicitly from Eqs. (21) to (23). Put differently, all contributions to Q^* except Eq. (26) constitute finite size corrections.

To summarize the self-consistency loop: starting from the mean-field autocorrelation Q^* we calculate the power spectrum of the single neuron activity based on Eq. (9) in frequency domain as $\langle\langle xx\rangle\rangle_*(\omega) = (Q^*(\omega)+D)/(1+\omega^2)$. This allows the calculation of $\langle\langle\phi^2(s,t)\rangle\rangle_*$, $\langle\phi'\rangle_*$ and the necessary cumulants of ϕ and $\tilde{x}$ for the β_{11} correction (27) using the results in Appendix C. Via Eq. (23) we can then calculate β_{11} and use Eq. (27) to close the loop for Q^*, iterating until convergence. In the linear case, we also take the β_{12} correction (28) into account which uses Eq. (21). The fluctuation

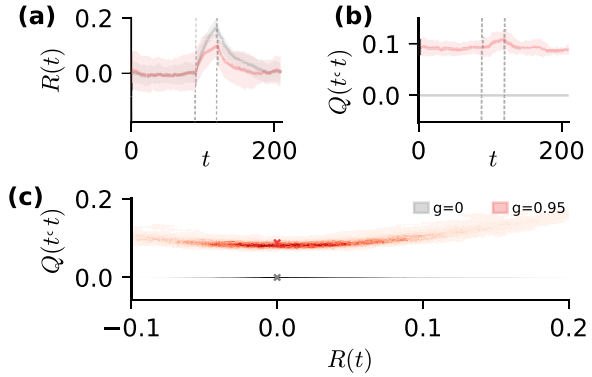

FIG. 4. (a) Transient of R in response to a stimulation provided as common input of 0.01 to each neuron [additive constant on right-hand side of Eq. (1)] within the time span indicated by the dashed lines; $\bar{g} = 1$ and different values of g ($g = 0$ in gray, $g = 0.95$ in red) with standard deviation across seeds (shaded). (b) Transient of Q under same conditions as in (a). (c) 2D histogram of Q over R with crosses at the zero time lag predicted as $Q^*(t,t)$ from theory (25). $\bar{g} = 1$, $g = 0$ in gray, $g = 0.95$ in red, other parameters as in Fig. 1.

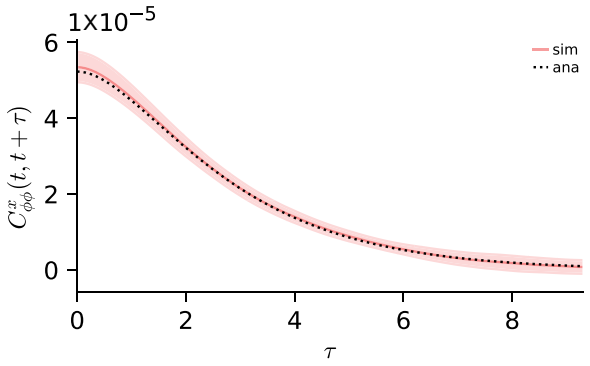

FIG. 5. Population averaged cross correlation $C^x_{\phi\phi}(\tau)$, Eq. (30), over time lag given by Eq. (30) (black) compared to simulation (red) with standard deviation from averaging over seeds (shaded) for $\bar{g} = 0.5$. Other parameters as in Fig. 1.

expansion (12) is equivalent to taking into account only the β_{11} correction and aborting after the first iteration.

III. RESULTS

For this section we consider the regime $g < 1$ and set $\phi(x) = \mathrm{erf}(\sqrt{\pi}x/2)$, which makes all expectation values of ϕ and its derivatives, which are necessary for the β_{11} correction (23), solvable analytically [28,31] while staying close to the popular choice of a hyperbolic tangent (for an explicit expression for Q^* including the contributions due to β_{12} in linear networks see Appendix D).

Figure 3 shows the autocorrelation for a network close to the phase transition. In the simulation results we observe the critical slowing down already visible in Fig. 1(c), which our self-consistent theory describes quite well. Above all, we see the emerging time constant corresponding to the decay of the network activities' autocorrelation $\beta_{11}(t-s) = \langle\langle R(t)R(s)\rangle\rangle$. Also the autocorrelation function features two different time scales: The fast time scale dominates the initial decay for time lags close to zero; this part is identical to the mean-field result neglecting fluctuations. The second time scale dominates the behavior of the autocorrelation function at large time lags. It is caused by the fluctuations of R as quantified by β_{11}. For an easier comparison, we also show an exponential decay with time constant $(1 - \bar{g}\langle\phi'\rangle)^{-1}$. As the average of ϕ' is only reliant on the zero time-lag statistics, we calculate it in mean-field approximation.

Figure 4 shows how a network's response to constant input changes close to the transition for different values of g. The population activity of a network with no variance in its connection ($g = 0$) behaves like a capacitor. For $g > 0$, the increase of the population activity due to the transient input is suppressed compared to $g = 0$. This highlights that close to the transition to the chaotic regime, a rise in the population-averaged activity R is counteracted by the increase of the variance measured by Q; formally this can be seen from the effective slope of the noise-averaged activation function [cf. Eq. (A1)] to decrease with increasing Q, which in turn reduces the positive feedback that controls the dynamics of R by Eq. (10). This stronger variability and the coupling of R and Q can be seen in Fig. 4(c) in the higher curvature for larger g. Our theory captures the resulting slightly elevated average of Q, as can be seen by the analytical crosses indicating $Q(\tau = 0)$ lying slightly above the parabolas' low points.

Direct access to Q and the fluctuations of R also allows us to conveniently calculate the pairwise averaged cross-correlation of the output

$$C^x_{\phi\phi}(t-s) := \frac{1}{N^2}\sum_{i\neq j}\phi_i(s)\phi_j(t) = \frac{\beta_{11}(s,t)}{\bar{g}^2} - \frac{Q(s,t)}{Ng^2}, \tag{30}$$

as can be seen in Fig. 5. Equation (30) highlights the large time constant $(1 - \bar{g}\langle\phi'\rangle)^{-1}$ present in the cross correlation induced by the network level correlation β_{11} which was also shown by Clark *et al.* [32] using cavity methods.

IV. DISCUSSION

In this paper we investigated the critical behavior close to the structured (ferromagnetic) regime of the Sompolinsky-Crisanti-Sommers model with nonzero mean connectivity and noise. After first reproducing the phase diagram using (dynamical) mean-field theory [16], we derive a self-consistent set of equations to one-loop order, systematically taking corrections of order $1/N$ into account. Our theory explains the emergence of long time scales in the decay of the population averaged autocorrelation function Q, which we show to be caused by fluctuations of the population-averaged population activity R. The theory furthermore links these network level effects to pairwise correlations on the single neuron scale. We thus successfully bridge between the emerging large time scales of the autocorrelation on the single neuron scale and finite size effects on the network level. Lastly, our analytical results explain how fluctuations of the population-averaged activity lead to a higher population averaged autocorrelation, showing a correlation in the two auxiliary fields that span

the phase space of recurrent networks and are conventionally studied in mean-field theory.

With regard to the study of criticality in neuronal networks, we have provided a model that features two critical transitions. First, the transition between the regular regime and the chaotic phase, which is predominantly controlled by the amount of disorder in the connectivity quantified by g and, in the absence of driving noise, indicated by the order parameter Q. This transition has been studied extensively in many previous works [7,11,33]. Our analysis here focuses on the "ferromagnetic" transition mainly controlled by the parameter $\bar{g}$, for which R plays the role of an order parameter. While our model focuses on a system out of equilibrium, the transition observed for $\bar{g} \simeq 1$ is comparable to the ferromagnetic transition of a classical Ising model. The dynamical model studied here reduces to an all-to-all coupled dynamical Ising model if one sets $g = 0$ and chooses a tanh nonlinearity for the neurons. Static counterparts of this model have been studied intensely in the form of maximum entropy models fitted to neural data like [34] where the instability of the population mode takes the role of the ferromagnetic transition. For $g \neq 0$, the dynamics of our model, however, becomes nonequilibrium. Still, the long time scale caused by the transition has the same origin as the critical slowing down observed in equilibrium counterparts of the model. Our theory explicitly demonstrates critical slowing down of the dynamics at the point of the continuous phase transition and allows the computation of the time scale. The theory, moreover, exposes that the two transitions cannot be studied in isolation, because we find a tight interplay of the two order parameters: fluctuations of R directly affect the order parameter Q, in particular the latter inherits the slow temporal decay from the critical fluctuations of the former. Also vice versa, the response of R is found to be multiphased, which appears to be caused by the back influence of Q on R.

On the side of network theory, the proposed method of a second-order Legendre transform to obtain a renormalized theory in the form of a set of self-consistency equations for the first and second-order statistics of the population activity may be useful to study other network properties. For example, within the framework of Bayesian inference [35,36], one cornerstone of contemporary theory of deep neuronal networks [37–39], the presented theory may be useful to compute the network prior. An interesting feature in this regard is that the neurons in our renormalized theory do not decouple, in contrast to the case of the large N-limit for deep and recurrent networks with centered prior distributions on the weights [40]. We hope that the presented framework will be useful to understand the functional consequences of this finding and that it will open the door to studying the finite-size properties of recurrent stochastic networks in continuous time in general.

ACKNOWLEDGMENTS

We are grateful for helpful discussions with A. Crisanti in the early stages of this project and T. Kühn for valuable feedback on the manuscript. This project has received funding from the European Union's Horizon 2020 Framework Programme for Research and Innovation under Specific Grant Agreement No. 945539 (Human Brain Project SGA3); the Helmholtz Association: Young investigator's Grant No. VH-NG-1028; the German Federal Ministry for Education and Research (BMBF Grant No. 01IS19077A to Jülich); Open access publication funded by the Deutsche Forschungsgemeinschaft (DFG, German Research Foundation) – 491111487. M.D. received funding as Vernetzungsdoktorand: "Dynamic characteristics of reservoir computing."

APPENDIX A: CRITICAL COUPLING STRENGTH IN MEAN-FIELD THEORY

We choose $\phi(x) = \mathrm{erf}(\sqrt{\pi}x/2)$, where the scaling ensures $\phi'(0) = 1$, for which the expectations on the r.h.s. of Eqs. (10) and (11) are solvable analytically [28, III.A.3]. In the stationary state, they are

$$\mu_\phi = \phi\left(\frac{\mu_x}{\sqrt{1+\frac{\pi}{2}\sigma_x^2}}\right), \tag{A1}$$

$$C_{\phi\phi}(\tau) = 1 - 8T\left(\frac{\sqrt{\frac{\pi}{2}}\mu_x}{\sqrt{1+\frac{\pi}{2}\sigma_x^2}}, \frac{\sqrt{1+\frac{\pi}{2}\sigma_x^2(1-\rho_x(\tau))}}{\sqrt{1+\frac{\pi}{2}\sigma_x^2(1+\rho_x(\tau))}}\right), \tag{A2}$$

with $\sigma_x^2 = C_x(0)$, $\rho_x(\tau) = C_x(\tau)/\sigma_x^2$, and Owen's T function $T(h,a) = \frac{1}{2\pi}\int_0^a dx\,(1+x^2)^{-1}e^{-\frac{1}{2}h^2(1+x^2)}$.

Inserting $\mu_x = \bar{g}\mu_\phi$ into Eq. (A1), we obtain

$$\mu_x = \bar{g}\,\phi\left(\frac{\mu_x}{\sqrt{1+\frac{\pi}{2}\sigma_x^2}}\right). \tag{A3}$$

Since $\phi(x)$ is sigmoidal and symmetric, Eq. (A3) has either one or three solutions—the latter corresponds to the state with a broken symmetry.

We approach the transition from the symmetric domain with $\mu_\phi = 0$. The deciding criterion to make multiple solutions possible is a unit slope at zero,

$$\frac{\bar{g}_c}{\sqrt{1+\frac{\pi}{2}\sigma_x^2}} = 1. \tag{A4}$$

For $\mu_x = 0$, Eq. (A2) simplifies to $C_{\phi\phi}(\tau) = \frac{2}{\pi}\arcsin y(\tau)$ where $y(\tau) = (1+\frac{\pi}{2}\sigma_x^2)^{-1}\frac{\pi}{2}\sigma_x^2\rho_x(\tau)$. This leads to the differential equation $\ddot{y} = -\partial_y V(y, y_0)$ with [41]

$$V(y,y_0) = -\tfrac{1}{2}y^2 + g^2(1-y_0)(\sqrt{1-y^2} + y\arcsin(y) - 1). \tag{A5}$$

Energy conservation determines the initial condition $y_0 = (1+\frac{\pi}{2}\sigma_x^2)^{-1}\frac{\pi}{2}\sigma_x^2$ and leads to $D = \frac{2}{\pi}(1-y_0)^{-1}\sqrt{-2V(y_0,y_0)}$. Using the stability criterion (A4) yields $y_0 = 1 - \bar{g}_c^{-2}$ and thus

$$D = \frac{2}{\pi}\bar{g}_c^2\sqrt{-2V(1-\bar{g}_c^{-2}, 1-\bar{g}_c^{-2})}, \tag{A6}$$

where the dependence on g is in $V(y,y_0)$. We obtained $D = D(\bar{g}_c, g^2)$ which can be solved numerically for $\bar{g}_c = \bar{g}_c(g,D)$.

For large time lag y tends to 0, allowing us to linearize the second-order differential equation to

$$\ddot{y} = (1 - g^2(1 - y_0))y + O(y^3),$$

where we can read off the time scale as

$$\tau_c = \sqrt{1 - g^2(1 - y_0)}^{-1}.$$

APPENDIX B: DOUBLE LEGENDRE TRANSFORMATION IN CUMULANTS

To derive the Legendre transformation in terms of cumulants, we restrict ourselves to a second-order transformation for brevity. We start by studying the properties of the effective action resulting from a first-order Legendre transformation to establish a ground truth. Then we will define the transformation in cumulants and compare its properties.

For the sake of keeping calculations concise we dress the second source term with a factor $\frac{1}{2}$ in the cumulant generating functional $W[j,k] = \ln \int_y \exp(S[y] + j^{\mathrm{T}}y + \frac{1}{2}y^{\mathrm{T}}ky)$ which gives us the moments

$$\alpha_1 = \langle y \rangle = \partial_j W,$$
$$\alpha_2 = \tfrac{1}{2}\langle y^2 \rangle = \partial_k W.$$

From here we continue to obtain the effective action

$$\Gamma_m[\alpha_1, \alpha_2] = \mathrm{extr}_{j,k}\, j^{\mathrm{T}}\alpha_1 + k^{\mathrm{T}}\alpha_2 - W[j,k],$$

which we decorated with a subscript m for "moment" to differentiate it from the effective action constructed via cumulants. While W defines an ensemble with fixed sources j and k which control the statistics of y, Γ_m instead defines an ensemble with fixed first and second moment of y, whose self-consistent values are obtained via the equations of state

$$\frac{\partial}{\partial \alpha_1}\Gamma_m[\alpha_1, \alpha_2] = j,$$
$$\frac{\partial}{\partial \alpha_2}\Gamma_m[\alpha_1, \alpha_2] = k.$$

Our goal now is to reformulate these expressions in terms of cumulants instead of moments. To this end we consider the definition of cumulants:

$$\beta_1 := \partial_j W = \langle y \rangle = \alpha_1,$$
$$\beta_2 := \partial_j^2 W = \langle y^2 \rangle - \langle y \rangle^2 = 2\alpha_2 - \alpha_1^2,$$

which can be inverted to yield

$$\alpha_1(\beta_1) = \beta_1,$$
$$\alpha_2(\beta_1, \beta_2) = \tfrac{1}{2}\big(\beta_2 + \beta_1^2\big).$$

This gives us a straightforward way of defining the Legendre transformation as a function of cumulants in terms of the standard Legendre transformation as a function of moments as

$$\Gamma_c[\beta_1, \beta_2] := \Gamma_m\big[\beta_1,\ \tfrac{1}{2}\big(\beta_2 + \beta_1^2\big)\big], \tag{B1}$$

and its equations of state

$$\begin{aligned}
\partial_{\beta_1}\Gamma_c[\beta_1, \beta_2] &= \partial_{\beta_1}\Gamma_m\big[\beta_1, \tfrac{1}{2}\big(\beta_2 + \beta_1^2\big)\big] \\
&= \underbrace{\partial_1\Gamma_m\big[\beta_1, \tfrac{1}{2}\big(\beta_2 + \beta_1^2\big)\big]}_{j} \\
&\quad + \underbrace{\partial_2\Gamma_m\big[\beta_1, \tfrac{1}{2}\big(\beta_2 + \beta_1^2\big)\big]}_{k}\beta_1 \\
&= j + \beta_1^{\mathrm{T}}k, \\
\partial_{\beta_2}\Gamma_c[\beta_1, \beta_2] &= \partial_{\beta_2}\Gamma_m\big[\beta_1, \tfrac{1}{2}\big(\beta_2 + \beta_1^2\big)\big] \\
&= \tfrac{1}{2}\underbrace{\partial_2\Gamma_m\big[\beta_1, \tfrac{1}{2}\big(\beta_2 + \beta_1^2\big)\big]}_{k} \\
&= \tfrac{1}{2}k,
\end{aligned}$$

in terms of the cumulants. Here ∂_1 and ∂_2 describe the derivative with respect to the first and second variable. To make the cumulant dependency more explicit we rewrite (B1):

$$\begin{aligned}
\Gamma_c[\beta_1, \beta_2] &= \mathrm{extr}_{j,k}\ -\ln \int_y e^{S[y] + j^{\mathrm{T}}y + \frac{1}{2}y^{\mathrm{T}}ky - j^{\mathrm{T}}\beta_1 - k^{\mathrm{T}}\frac{1}{2}\left(\beta_2 + \beta_1^2\right)} \\
&= \mathrm{extr}_{j,k} - \ln \int_y e^{S[y] + (j + k^{\mathrm{T}}\beta_1)^{\mathrm{T}}(y - \beta_1) + \frac{k^{\mathrm{T}}}{2}\left((y - \beta_1)^2 - \beta_2\right)}.
\end{aligned}$$

By introducing $\hat{j} := j + k^{\mathrm{T}}\beta_1$ we keep the form of the stationarity equation with $\frac{\partial}{\partial \hat{j}}$ applied to the right-hand side yielding zero. Both pairs of stationarity conditions $\{\partial/\partial j, \partial/\partial k\}$ and $\{\partial/\partial \hat{j}, \partial/\partial k\}$ imply the same pair of constraints because the only additional term produced by $\partial/\partial k$ acting on $(k^{\mathrm{T}}\beta_1)^{\mathrm{T}}(y - \beta_1)$ is proportional to $\langle y - \beta_1 \rangle$ which, as a result of the constraint enforced by $\partial/\partial j$, vanishes. We can thus write the effective action for cumulants as

$$\Gamma_c[\beta_1, \beta_2] = \mathrm{extr}_{\hat{j},k}\ -\ln \int_y e^{S[y] + \hat{j}^{\mathrm{T}}(y - \beta_1) + \frac{k^{\mathrm{T}}}{2}((y - \beta_1)^2 - \beta_2)}, \tag{B2}$$

with

$$\partial_{\hat{j}}\Gamma_c[\beta_1, \beta_2] = 0,$$
$$\partial_k\Gamma_c[\beta_1, \beta_2] = 0,$$
$$\partial_{\beta_1}\Gamma_c[\beta_1, \beta_2] = j + \beta_1^{\mathrm{T}}k,$$
$$\partial_{\beta_2}\Gamma_c[\beta_1, \beta_2] = \tfrac{1}{2}k.$$

We have thus found a way to describe a system in terms of cumulants.

APPENDIX C: FACTORING ϕ-EXPECTATION VALUES

In this chapter we show how to calculate $\langle \prod_i^n \tilde{x}(s_i) \prod_j^m \phi(x(t_j)) \rangle$ under a Gaussian measure, which we need to solve our self-consistent equations. We will do so inspired by the derivations of Price theorem [42]. This means we express ϕ via their Fourier representation and pull everything except the exponential necessary for this transformation outside of the expectation value. Doing so comes at the cost of having to calculate some derivatives, but this enables us to perform the integration for the expectation values and in the end clean up by calculating said derivatives.

The first step is the Fourier representation and insertion of a source term for $\tilde{x}$. We then replace $\tilde{x}$ by derivatives with respect to this source, allowing us to rewrite $\langle \prod_i^n \tilde{x}(s_i) \prod_j^m \phi(x(t_j)) \rangle$ as

$$\prod_j \left\{ \int dk_j \hat{\phi}(k_j) \right\} \left\langle \prod_i \{\tilde{x}(s_i)\} \exp\left(\mathrm{i} \sum_j \mathbf{k}_j x(t') dt' \right) \right\rangle = \prod_j \left\{ \int dk_j \hat{\phi}(k_j) \right\} \left[\prod_i \{-\mathrm{i}\delta_{\tilde{k}(s_i)}\} \underbrace{\left\langle \exp(\mathrm{i} \sum_j \mathbf{k}_j x(t') dt' + \mathrm{i}\tilde{k}\tilde{x}) \right\rangle}_{(\star)} \right]_{\tilde{k}=0} . \tag{C1}$$

There we used the abbreviations $\mathbf{k}_j := \int 2\pi k_j \delta(t_j - t')$. From here we focus on the expectation value denoted by $\star$ which we write out as an integration over x and $\tilde{x}$ w.r.t. their distribution function. We assume the fields to be distributed according to a Gaussian with covariance

$$\Delta = \begin{pmatrix} \Delta_{xx} & \Delta_{x\tilde{x}} \\ \Delta_{x\tilde{x}}^* & 0 \end{pmatrix}.$$

Here it is important to note that $\tilde{x}$ is a response field and therefore has a vanishing autocorrelation, allowing us to set $\Delta_{\tilde{x}\tilde{x}} = 0$. The resulting integrand is an exponential of a quadratic polynomial, which we solve using a Hubbard-Stratonovich transformation:

$$\begin{aligned} (\star) &= \int dx\, d\tilde{x} \exp\left(-\frac{1}{2} \begin{pmatrix} x \\ \tilde{x} \end{pmatrix}^{\mathrm{T}} \Delta^{-1} \begin{pmatrix} x \\ \tilde{x} \end{pmatrix} + \mathrm{i}x \sum_j \mathbf{k}_j + \mathrm{i}\tilde{k}\tilde{x} \right) \\ &= \exp\left(-\frac{1}{2} \begin{pmatrix} \sum \mathbf{k}_j \\ \tilde{k} \end{pmatrix}^{\mathrm{T}} \Delta \begin{pmatrix} \sum \mathbf{k}_j \\ \tilde{k} \end{pmatrix} \right) \\ &=: \exp(D(\tilde{k})). \end{aligned}$$

Plugging this back into Eq. (C1), we see that the derivatives we need to calculate are $\prod_i \{\delta_{\tilde{k}(s_i)}\} \exp(D(\tilde{k}))$. As $D(\tilde{k})$ is just a quadratic equation, we can easily calculate its first two derivatives:

$$\begin{aligned} \delta_{\tilde{k}(s_i)} D(\tilde{k}) &= D'(\tilde{k})(s_i) \\ &= -\begin{pmatrix} 0 \\ 1 \end{pmatrix}^{\mathrm{T}} \Delta \begin{pmatrix} \sum_j \mathbf{k}_j \\ \tilde{k} \end{pmatrix} \\ &= -\int_{t'} \Delta_{x\tilde{x}}(s_i, t') \sum_j \mathbf{k}_j \\ &= -\sum_j \Delta_{x\tilde{x}}(s_i, t_j) k_j \\ \Rightarrow D''(\tilde{k}) &= 0. \end{aligned}$$

Thus it can be shown by induction:

$$\prod_i \{\delta_{\tilde{k}(t_i)}\} \exp(D(\tilde{k})) = \exp(D(\tilde{k})) \prod_i D'(\tilde{k})(s_i)$$

with base case

$$\begin{aligned} \exp(D(0)) &= \exp\left(-\frac{1}{2} \sum \mathbf{k}_j \Delta_{11} \sum \mathbf{k}_j \right) \\ &= \int dx\, d\tilde{x} \exp\left(-\frac{1}{2} \begin{pmatrix} x \\ \tilde{x} \end{pmatrix}^{\mathrm{T}} \Delta^{-1} \begin{pmatrix} x \\ \tilde{x} \end{pmatrix} + \mathrm{i}x \sum_j \mathbf{k}_j \right) \\ &= \left\langle \exp\left(\mathrm{i}x \sum_j \mathbf{k}_j \right) \right\rangle \\ &= \left\langle \prod_j \exp(\mathrm{i}x\mathbf{k}_j) \right\rangle \\ &= \left\langle \prod_j \exp(\mathrm{i}\, k_j\, x(t_j)) \right\rangle. \end{aligned}$$

This way we get

$$\left\langle \prod_i^n \tilde{x}(s_i) \prod_j^m \phi(x(t_j)) \right\rangle = \left\langle \prod_j \left\{ \int dk_j \hat{\phi}(k_j) \exp(\mathrm{i}\, k_j\, x(t_j)) \right\} \right\rangle \cdot \underbrace{\prod_i^n \sum_j^m \Delta_{x\tilde{x}}(s_i, t_j) \mathrm{i} k_j}_{(\star\star)} .$$

To simplify this further, we want to perform the k_j integrals but for this need to rewrite the term denoted by $(\star\star)$. One way of doing this would be

$$\begin{aligned} (\star\star) &= \left(\sum_{j_1}^m \Delta_{x\tilde{x}}(s_1, t_{j_1}) \mathrm{i} k_{j_1} \right) \ldots \left(\sum_{j_n}^m \Delta_{x\tilde{x}}(s_n, t_{j_n}) \mathrm{i} k_{j_n} \right) \\ &= \sum_{\boldsymbol{j}} \prod_i^n \Delta_{x\tilde{x}}(s_i, t_{j_i}) \mathrm{i} k_{j_i}. \end{aligned}$$

Even though this makes it very cumbersome to perform the integral, as the multi-indexed k can be part of any integral, this form lets us see how the final result will look like: each term of the sum has to have one factor $\prod_j k_j^{\alpha_j}$ with $\sum_j \alpha_j = n$. This is then multiplied by a sum of products of $\Delta_{x\tilde{x}}(s_i, t_j)$, where each j appears as often in each product as the value of α_j and the i takes all values from 1 to n. The sum then goes over all

different combinations of i and j. So we introduce

$$j(\alpha) = (\underbrace{1,\dots,1}_{\alpha_1\text{times}}, \underbrace{2\dots,2}_{\alpha_2\text{times}}, \underbrace{3,\dots,3}_{\alpha_3\text{times}}, \dots),$$
$$j(\alpha, i) = (j(\alpha))_i,$$

and the permutation group S, which does not switch the j's, which are equal. Doing so allows us to finally rewrite $\langle\prod_i^n \tilde{x}(s_i)\prod_j^m \phi(x(t_j))\rangle$:

$$\left\langle \prod_j \left\{ \int dk_j \hat{\phi}(k_j) \exp(\mathrm{i}\, k_j\, x(t_j)) \right\} \right\rangle \cdot \sum_{\alpha,\sum_j \alpha_j = n} \prod_j \left\{ (\mathrm{i}k_j)^{\alpha_j} \right\} \sum_{\sigma\in S} \prod_i \Delta_{x\tilde{x}}(s_i, t_{\sigma(j(\alpha,i))})$$
$$= \sum_{\alpha,\sum_j \alpha_j = n} \left\langle \prod_j \left\{ \int dk_j (\mathrm{i}k_j)^{\alpha_j} \hat{\phi}(k_j) \exp(\mathrm{i}\, k_j\, x(t_j)) \right\} \right\rangle \cdot \sum_{\sigma\in S} \prod_i \Delta_{x\tilde{x}}(s_i, t_{\sigma(j(\alpha,i))})$$
$$= \sum_{\alpha,\sum_j \alpha_j = n} \left\langle \prod_j \left\{ \phi^{(\alpha_j)}(x(t_j)) \right\} \right\rangle \sum_{\sigma\in S} \prod_i \Delta_{x\tilde{x}}(s_i, t_{\sigma(j(\alpha,i))}).$$

For the relevant cases this results in

$$\begin{aligned}
\langle\langle \phi(t)\phi(s), \tilde{x}(u), \tilde{x}(v)\rangle\rangle &= \langle \phi^2(s,t)\tilde{x}(u)\tilde{x}(v)\rangle \\
&= \langle \phi''(s)\phi(t)\rangle\langle\tilde{x}(u)x(s)\rangle\langle\tilde{x}(v)x(s)\rangle + \langle\phi''(t)\phi(s)\rangle\langle\tilde{x}(u)x(t)\rangle\langle\tilde{x}(v)x(t)\rangle \\
&\quad + \langle\phi'(s)\phi'(t)\rangle(\langle\tilde{x}(u)x(t)\rangle\langle\tilde{x}(v)x(s)\rangle + \langle\tilde{x}(u)x(s)\rangle, \langle\tilde{x}(v)x(t)\rangle), \\
\langle\langle \phi(t)\phi(s), \tilde{x}(u), \phi(v)\rangle\rangle &= \langle\phi(s)\phi(t)\tilde{x}(u)\phi(v)\rangle - \langle\phi(s)\phi(t)\rangle\langle\tilde{x}(u)\phi(v)\rangle \\
&= \langle\phi'(s)\phi(t)\phi(v)\rangle\langle\tilde{x}(u)x(s)\rangle + \langle\phi'(t)\phi(s)\phi(v)\rangle\langle\tilde{x}(u)x(t)\rangle \\
&\quad + \langle\phi'(v)\phi(s)\phi(t)\rangle\langle\tilde{x}(u)x(v)\rangle\langle\phi'\rangle - \langle\phi(s)\phi(t)\rangle\langle\tilde{x}(u)\phi(v)\rangle \\
\langle\langle \phi(t)\phi(s), \phi(u), \tilde{x}(v)\rangle\rangle &= \langle\phi(s)\phi(t)\phi(u)\tilde{x}(v)\rangle - \langle\phi(s)\phi(t)\rangle\langle\tilde{x}(v)\phi(u)\rangle \\
&= \langle\phi'(s)\phi(t)\phi(u)\rangle\langle\tilde{x}(v)x(s)\rangle + \langle\phi'(t)\phi(s)\phi(u)\rangle\langle\tilde{x}(v)x(t)\rangle \\
&\quad + \langle\phi'(u)\phi(s)\phi(t)\rangle\langle\tilde{x}(v)x(u)\rangle - \langle\phi(s)\phi(t)\rangle\langle\tilde{x}(v)x(u)\rangle\langle\phi'\rangle.
\end{aligned}$$

As the response function is known in the Fourier domain as $-1/(1+i\omega)$, this only leaves the expectation values of products of derivatives of ϕ to be calculated. For the case where only β_{11} corrections are considered these are $\langle\phi(s)\phi(t)\rangle$, $\langle\phi''(s)\phi(t)\rangle$ and $\langle\phi'(s)\phi'(t)\rangle$. The expectation values $\langle f(x(s))g(x(t))\rangle$ are taken over x, so we can express them as Gaussian integrals

$$\langle f(y)g(z)\rangle = \int dy\, dz\, f(y)\, g(z) \exp\left(-\frac{1}{2}(y,z)C_\tau^{-1}(y,z)^{\mathrm{T}}\right)\sqrt{|C_\tau|}^{-1},$$
$$\text{with } C_\tau = \begin{pmatrix} c_0 & c(\tau) \\ c(\tau) & c_0 \end{pmatrix},$$

where we defined $c_0 = \langle xx\rangle(0)$ and $c(\tau) = \langle xx\rangle(\tau)$ with $\tau = t - s$. In the case of $\phi(x) = \mathrm{erf}(\sqrt{\pi}x/2)$ these integrals can be evaluated with the help of Owen [31], resulting in

$$\langle\phi\phi\rangle(\tau) = \frac{2}{\pi}\arcsin\left(\frac{\pi c(\tau)}{2+\pi c_0}\right),$$
$$\langle\phi'\phi'\rangle(\tau) = \sqrt{\left(1+\frac{\pi c_0}{2}\right)^2 - \left(\frac{\pi c(\tau)}{2}\right)^2}^{-1},$$
$$\langle\phi''\phi\rangle(\tau) = -\pi c(\tau)\frac{\langle\phi'\phi'\rangle(\tau)}{2+\pi c_0}.$$

APPENDIX D: ANALYTICAL RESULTS FOR LINEAR ACTIVATION FUNCTION

Here we consider the case $\phi(x) = x$. First we calculate $\langle xx\rangle_*(\omega)$ via Eq. (9) by transforming to Fourier domain, multiplying the equation with itself and taking the expectation value leading to

$$\langle xx\rangle_*(\omega) = \frac{Q^*(\omega) + D}{1+\omega^2}. \tag{D1}$$

At the saddle point we have $Q^* = g^2\langle xx\rangle$ and are thus able to solve

$$\langle xx\rangle_*(\omega) = \frac{D}{1-g^2+\omega^2},$$
$$\langle xx\rangle_*(\tau) = \frac{D}{\sqrt{1-g^2}}\exp(-|\tau|\sqrt{1-g^2}), \tag{D2}$$

where we took the Fourier transform in the last step. Here we can see the time constant $\sqrt{1-g^2}^{-1}$ in the mean-field solution, which is independent of $\bar{g}$.

We can, however, go further than mean field and derive an explicit solution for the first equation of state (25):

$$\begin{aligned} Q^*(s,t) &= g^2\langle\langle x^2\rangle\rangle_*(s,t) \\ &\quad + \frac{1}{2}g^2\int_{u,v}\langle\langle x^2(s,t),\tilde{x}(u),\tilde{x}(v)\rangle\rangle_*\beta_{11}(u,v) \\ &\quad + g^2\bar{g}\int_{u,v}\langle\langle x^2(s,t),\tilde{x}(u),x(v)\rangle\rangle_*\beta_{12}(u,v). \end{aligned} \tag{D3}$$

For this we need values for the second cumulant of the auxiliary fields and particular third cumulants of the single neuron dynamic. To get the former we use the first equation of state (25) in Fourier domain

$$\beta_{12}(\omega) = \frac{1}{N}\frac{1+i\omega}{1-\bar{g}+i\omega}, \tag{D4}$$
$$\begin{aligned} \beta_{11}(\omega) &= N\beta_{12}(\omega)\langle xx\rangle_*(\omega)\beta_{21}(\omega) \\ &= \frac{1}{N}\frac{Q^*(\omega)+D}{(1-\bar{g})^2+\omega^2}, \end{aligned} \tag{D5}$$

where we used Eq. (D1) in the last line. The latter we can break down into second moments via the methods derived in Appendix C:

$$\begin{aligned} \langle\langle x(t)x(s),\tilde{x}(u),\tilde{x}(v)\rangle\rangle_* &= \langle\tilde{x}(u)x(t)\rangle\langle\tilde{x}(v)x(s)\rangle \\ &\quad + \langle\tilde{x}(u)x(s)\rangle,\langle\tilde{x}(v)x(t)\rangle \\ \langle\langle x(t)x(s),\tilde{x}(u),x(v)\rangle\rangle_* &= \langle x(t)x(v)\rangle\langle\tilde{x}(u)x(s)\rangle \\ &\quad + \langle x(s)x(v)\rangle\langle\tilde{x}(u)x(t)\rangle. \end{aligned}$$

As we will solve the integrals in the Fourier domain, it is easiest to name them:

$$\begin{aligned} I_{11}(s-t) &= \frac{g^2}{2}\int du\,dv\,\langle\langle x(t)x(s),\tilde{x}(u),\tilde{x}(v)\rangle\rangle_*\beta_{11}(u-v) \\ &= g^2\int du\,dv\,\langle\tilde{x}(u)x(s)\rangle_*\langle\tilde{x}(v)x(t)\rangle_*\beta_{11}(u-v). \end{aligned}$$

This leaves us with a double convolution which turns into a product in Fourier domain:

$$\begin{aligned} g^{-2}I_{11}(\tau) &= \int\frac{d\omega}{2\pi}\langle\tilde{x}x\rangle(\omega)\langle\tilde{x}x\rangle_*(-\omega)\beta_{11}(-\omega)\exp(i\omega(\tau)) \\ &= \int\frac{d\omega}{2\pi}\frac{\beta_{11}(\omega)}{1+\omega^2}\exp(i\omega(\tau)) \\ &= \int\frac{d\omega}{2\pi}\frac{1}{N}\frac{Q(\omega)+D}{(1-\bar{g})^2+\omega^2}\frac{1}{1+\omega^2}\exp(i\omega(\tau)) \\ &= \int\frac{d\omega}{2\pi}I_{11}(\omega)\exp(i\omega(\tau)), \end{aligned}$$

whereby we used again the evenness of β_{11} and the shape of the activity's response function in Fourier domain $\langle\tilde{x}x\rangle(\omega) = -(1+i\omega)^{-1}$.

We can deal with the second integral equivalently:

$$\begin{aligned} \frac{I_{12}(s-t)}{g^2\bar{g}} &= \int_{u,v}\langle\langle x^2(s,t),\tilde{x}(u),x(v)\rangle\rangle_*\beta_{12}(u,v) \\ &= \int_{u,v}(\langle x(t)x(v)\rangle\langle\tilde{x}(u)x(s)\rangle \\ &\quad + \langle x(s)x(v)\rangle\langle\tilde{x}(u)x(t)\rangle)\beta_{12}(u,v) \\ &= \int_{u,v}(\langle xx\rangle(v-t)\langle\tilde{x}x\rangle(s-u) \\ &\quad + \langle xx\rangle(v-s)\langle\tilde{x}x\rangle(t-u))\beta_{12}(u,v) \\ &= \int\frac{d\omega}{2\pi}\exp(i\omega(s-t)) \\ &\quad \frac{1}{N}\frac{1-\bar{g}+\omega^2(1+\bar{g})}{(1-\bar{g})^2+\omega^2}\frac{-2}{1+\omega^2}\langle xx\rangle_*(\omega), \end{aligned}$$

and thus get

$$I_{11}(\omega) = \frac{g^2}{N}\frac{Q(\omega)+D}{(1-\bar{g})^2+\omega^2}\frac{1}{1+\omega^2},$$
$$I_{12}(\omega) = -\frac{2g^2\bar{g}}{N}\frac{Q(\omega)+D}{(1+\omega^2)^2}\frac{1-\bar{g}+\omega^2(1+\bar{g})}{(1-\bar{g})^2+\omega^2}.$$

From here we can solve for $Q(\omega)$:

$$\begin{aligned} Q(\omega) &= \int\frac{d\omega}{2\pi}Q(\tau_1)\exp(i\omega\tau_1) \\ &= g^2\langle xx\rangle_1(\omega) + I_{11}(\omega) + I_{12}(\omega) \\ &= \frac{Q(\omega)+D}{1+\omega^2}\alpha(\omega) \\ \Leftrightarrow Q(\omega) &= D\frac{\alpha(\omega)}{1-\alpha(\omega)+\omega^2} \end{aligned}$$

with

$$\begin{aligned} \alpha(\omega) &= g^2\Bigg(1+\frac{1}{N}\frac{1}{(1-\bar{g})^2+\omega^2} \\ &\quad - \frac{1}{N}\frac{2\bar{g}}{1+\omega^2}\frac{1-\bar{g}+\omega^2(1+\bar{g})}{(1-\bar{g})^2+\omega^2}\Bigg) \\ &= g^2\Bigg(1+\frac{1}{N}\frac{1}{(1-\bar{g})^2+\omega^2} \\ &\quad \times\left[1-2\bar{g}(1+\bar{g}-\frac{2}{1+\omega^2})\right]\Bigg). \end{aligned}$$

The first term $\alpha(\omega) = g^2$ without finite-size corrections reproduces the mean-field result of an exponentially decaying autocorrelation with time constant $\sqrt{1-g^2}^{-1}$. The correction terms show the time constant $(1-\bar{g})^{-1}$.

[1] J. M. Beggs and D. Plenz, Neuronal avalanches are diverse and precise activity patterns that are stable for many hours in cortical slice cultures, J. Neurosci. **24**, 5216 (2004).

[2] D. R. Chialvo, Emergent complex neural dynamics, Nat. Phys. **6**, 744 (2010).

[3] V. Priesemann, M. Wibral, M. Valderrama, R. Pröpper, M. Le Van Quyen, T. Geisel, J. Triesch, D. Nikolic, and M. H. J. Munk, Spike avalanches *in vivo* suggest a driven, slightly subcritical brain state, Front. Syst. Neurosci. **8**, 80 (2014).

[4] A. J. Fontenele, N. A. P. de Vasconcelos, T. Feliciano, L. A. A. Aguiar, C. Soares-Cunha, B. Coimbra, L. Dalla Porta, S. Ribeiro, A. J. Rodrigues, N. Sousa, P. V. Carelli, and M. Copelli, Criticality between cortical states, Phys. Rev. Lett. **122**, 208101 (2019).

[5] N. Goldenfeld, *Lectures on Phase Transitions and the Renormalization Group* (Perseus books, Reading, MA, 1992).

[6] T. Toyoizumi and L. F. Abbott, Beyond the edge of chaos: Amplification and temporal integration by recurrent networks in the chaotic regime, Phys. Rev. E **84**, 051908 (2011).

[7] J. Schuecker, S. Goedeke, and M. Helias, Optimal sequence memory in driven random networks, Phys. Rev. X **8**, 041029 (2018).

[8] R. Legenstein and W. Maass, Edge of chaos and prediction of computational performance for neural circuit models, Neural Networks **20**, 323 (2007).

[9] J. Kadmon and H. Sompolinsky, Transition to chaos in random neuronal networks, Phys. Rev. X **5**, 041030 (2015).

[10] D. Dahmen, S. Grün, M. Diesmann, and M. Helias, Second type of criticality in the brain uncovers rich multiple-neuron dynamics, Proc. Natl. Acad. Sci. USA **116**, 13051 (2019).

[11] H. Sompolinsky, A. Crisanti, and H. J. Sommers, Chaos in random neural networks, Phys. Rev. Lett. **61**, 259 (1988).

[12] J. M. Beggs and D. Plenz, Neuronal avalanches in neocortical circuits, J. Neurosci. **23**, 11167 (2003).

[13] T. Tao, Outliers in the spectrum of iid matrices with bounded rank perturbations, Probab. Theory Relat. Fields **155**, 231 (2013).

[14] F. Schuessler, A. Dubreuil, F. Mastrogiuseppe, S. Ostojic, and O. Barak, Dynamics of random recurrent networks with correlated low-rank structure, Phys. Rev. Res. **2**, 013111 (2020).

[15] F. Mastrogiuseppe and S. Ostojic, Linking connectivity, dynamics, and computations in low-rank recurrent neural networks, Neuron **99**, 609 (2018).

[16] F. Mastrogiuseppe and S. Ostojic, Intrinsically-generated fluctuating activity in excitatory-inhibitory networks, PLoS Comput. Biol. **13**, e1005498 (2017).

[17] C. van Vreeswijk, Partial synchronization in populations of pulse-coupled oscillators, Phys. Rev. E **54**, 5522 (1996).

[18] D. J. Amit and N. Brunel, Model of global spontaneous activity and local structured activity during delay periods in the cerebral cortex, Cereb. Cortex **7**, 237 (1997).

[19] N. Brunel, Dynamics of sparsely connected networks of excitatory and inhibitory spiking neurons, J. Comput. Neurosci. **8**, 183 (2000).

[20] A. Vasiliev, *Functional Methods in Quantum Field Theory and Statistical Physics* (Gordon and Breach Science Publishers, London, 1998).

[21] J. Berges, Introduction to nonequilibrium quantum field theory, AIP Conf. Proc. **739**, 3 (2004).

[22] P. Martin, E. Siggia, and H. Rose, Statistical dynamics of classical systems, Phys. Rev. A **8**, 423 (1973).

[23] H.-K. Janssen, On a Lagrangean for classical field dynamics and renormalization group calculations of dynamical critical properties, Z. Phys. B **23**, 377 (1976).

[24] C. De Dominicis, Techniques de renormalisation de la théorie des champs et dynamique des phénomènes critiques, J. Phys. Colloques **37**, C1-247 (1976).

[25] C. Chow and M. Buice, Path integral methods for stochastic differential equations, J. Math. Neurosci. **5**, 8 (2015).

[26] J. A. Hertz, Y. Roudi, and P. Sollich, Path integral methods for the dynamics of stochastic and disordered systems, J. Phys. A **50**, 033001 (2017).

[27] M. Helias and D. Dahmen, *Statistical Field Theory for Neural Networks* (Springer International Publishing, New York, 2020), p. 203.

[28] A. van Meegen and S. J. van Albada, Microscopic theory of intrinsic timescales in spiking neural networks, Phys. Rev. Res. **3**, 043077 (2021).

[29] J. Zinn-Justin, *Quantum Field Theory and Critical Phenomena* (Clarendon Press, Oxford, 1996).

[30] M. Mézard, G. Parisi, and M. Virasoro, *Spin Glass Theory and Beyond: An Introduction to the Replica Method and Its Applications*, Lecture Notes in Physics (World Scientific Publishing Company, Singapore, 1987), Vol. 9.

[31] D. B. Owen, A table of normal integrals, Commun. Stat. Simul. Comput. **9**, 389 (1980).

[32] D. G. Clark, L. F. Abbott, and A. Litwin-Kumar, Dimension of activity in random neural networks, Phys. Rev. Lett. **131**, 118401 (2023).

[33] D. Martí, N. Brunel, and S. Ostojic, Correlations between synapses in pairs of neurons slow down dynamics in randomly connected neural networks, Phys. Rev. E **97**, 062314 (2018).

[34] G. Tkacik, T. Mora, O. Marre, D. Amodei, S. E. Palmer, M. J. Berry, and W. Bialek, Thermodynamics and signatures of criticality in a network of neurons, Proc. Natl. Acad. Sci. USA **112**, 11508 (2015).

[35] C. K. Williams, Computation with infinite neural networks, Neural Comput. **10**, 1203 (1998).

[36] J. Lee, J. Sohl-Dickstein, J. Pennington, R. Novak, S. Schoenholz, and Y. Bahri, Deep neural networks as Gaussian processes, in *International Conference on Learning Representations* (OpenReview.net, Vancouver, Canada, 2018).

[37] J. A. Zavatone-Veth and C. Pehlevan, Exact marginal prior distributions of finite Bayesian neural networks, in *Advances in Neural Information Processing Systems*, edited by A. Beygelzimer, Y. Dauphin, P. Liang, and J. W. Vaughan (NeurIPS, Virtual, 2021).

[38] J. A. Zavatone-Veth, A. Canatar, B. Ruben, and C. Pehlevan, Asymptotics of representation learning in finite Bayesian neural networks, in *Advances in Neural Information Processing Systems*, edited by A. Beygelzimer, Y. Dauphin, P. Liang, and J. W. Vaughan (NeurIPS, Virtual, 2021).

[39] I. Seroussi, G. Naveh, and Z. Ringel, Separation of scales and a thermodynamic description of feature learning in some cnns, Nat. Commun. **14**, 908 (2023).

[40] K. Segadlo, B. Epping, A. van Meegen, D. Dahmen, M. Krämer, and M. Helias, Unified field theoretical approach to deep and recurrent neuronal networks, J. Stat. Mech. (2022) 103401.

[41] A. van Meegen, T. Kühn, and M. Helias, Large-deviation approach to random recurrent neuronal networks: Parameter inference and fluctuation-induced transitions, Phys. Rev. Lett. **127**, 158302 (2021).

[42] A. Papoulis, *Probability, Random Variables, and Stochastic Processes*, 3rd ed. (McGraw-Hill, Boston, MA, 1991).